Administered Activity Optimization in ^{99m}Tc-MAG3 Renography for Adults

Marlén P. Díaz, MSc[1]; Eric E. Aparicio, MSc[2]; Oscar D. Rizo, PhD[3]; Reinaldo R. Díaz, BSc[2]; and Carlos H. Rodríguez, MD[2]

[1]Central University of Las Villas, Santa Clara, Cuba; [2]University Hospital "Celestino Hdez Robau," Santa Clara, Cuba; and [3]Institute for Nuclear Sciences and Technology, Havana, Cuba

Objective: The objective of this work was to determine the minimum administered activity of ^{99m}Tc-mercaptoacetyltriglycine (MAG3) needed both to estimate effective renal plasma flow (ERPF) with adequate precision and to obtain good image quality.

Methods: Three groups of 10 patients each were injected with 45, 71, or 132 MBq of MAG3. Renograms and perfusion and clearance images were obtained. The age, sex, and weight of the patients; the labeling yield; the mean count and counting rate 2 min after injection; the kidney-to-background and cortex-to-background ratios; the uptake time from the renograms; the percentage of the injected activity 2 min after injection in the left and right kidneys ($A2_{LK}$ and $A2_{RK}$, respectively); and the ERPF for both kidneys were obtained and analyzed. Discriminant analysis of image quality was used to select the variables that most affected image quality. The selected variables were studied among activity groups to optimize the amount of activity administered in these studies.

Results: Precision in ERPF assessment did not significantly differ among administered activity levels ($P = 0.824$). The SDs of the ERPF were ± 1.5 for 132 MBq, ± 1.7 for 71 MBq, and ± 2.0 for 45 MBq. The labeling yield, the ratios of counts in the left and right kidneys to the background and in the left and right cortices to the background, and $A2_{LK}$ and $A2_{RK}$ were the only variables that provided a significant discriminant function for image quality. The only variable that significantly differed with the variation in administered activity was the ratio of counts in the right kidney to the background ($P = 0.026$), most likely because of the labeling yield.

Conclusion: A 45-MBq activity is sufficient to guarantee good image quality and adequate precision in ERPF determination from the time–activity curve, provided the labeling yield is kept high.

Key Words: activity optimization; ^{99m}Tc-MAG3; discriminant analysis; image quality; patient dose

J Nucl Med Technol 2003; 31:216–221

For correspondence or reprints contact: Marlén Pérez Díaz, MSc, Physics Department, Central University of Las Villas, Camajuani Rd., Km. 5½, Santa Clara 53840, Villa Clara, Cuba.
E-mail: mperez@mfc.uclv.edu.cu

$\mathbf{T}$he amount of activity administered to patients is an important aspect of nuclear medicine studies that is now being investigated. The aim is to find a compromise between image quality and radiation risk to the patient. The activity administered in the different types of studies varies among centers and countries. One important step to the achievement of a standardized value is the introduction of reference levels (*1*), based mainly on the current statistical distributions of administered activity. The amount used in each clinic depends on the radiopharmaceutical choice, equipment characteristics, matrix size, patient size, acquisition time, and study type (static, dynamic, or SPECT) (*2*). Thus, it is important to study how the administered activity influences diagnostic precision in each specific context.

Moonen and Jacobsson (*3*) simulated varying activity levels by adding different amounts of random statistical noise. They analyzed how the administered activity influenced precision in the measurement of effective renal plasma flow (ERPF), the main parameter determined in γ-camera renograms. Vestergren et al. (*4*) validated the biokinetic model of Moonen et al. (*5*) for uptake and excretion of hippuran to ^{99m}Tc-mercaptoacetyltriglycine (MAG3). They used this result to calculate the value of the administered activity for children as a fraction of the activity for adults. They corroborated Moonen and Jacobson's result—that, instead of the more commonly used value of 100 MBq, 45 MBq (1.2 mCi) obtains adequate precision in the determination of ERPF in adults.

The objective of this work was to use a discriminant mathematic tool to determine the administered activity for ^{99m}Tc-MAG3 renal studies that would best provide good image quality, adequate precision in ERPF determination, and radiation safety for patients.

MATERIALS AND METHODS

Patient Population

A random sample of 30 patients (9 male and 21 female) undergoing routine γ-camera renography was selected. Informed consent was obtained from all participants before any test was performed. Age ranged from 18 to 74 y, with

an average of 41.4 ± 14.8 y; weight ranged from 41 to 123 kg, with an average of 66.2 ± 18.5 kg; and height ranged from 148 to 179 cm, with an average of 165.3 ± 8.4 cm. Table 1 shows the patient characteristics and a statistical analysis among groups.

Preparation of Injections

MAG3 was labeled with ^{99m}Tc-pertechnetate obtained from the molybdenum–technetium morning elution. The main labeling yield was determined in each case by ascendant chromatography, using a 2:3:13 system of acetic acid:chloroform:acetone. The samples were measured in a well scintillation detector (model 20046; Robotron) calibrated for the ^{99m}Tc energy. The mean labeling yield was $92.7\% \pm 1.7\%$.

Patients were assigned into 3 groups of 10 patients each. ^{99m}Tc-MAG3 in activities of 45 ± 2 MBq (1.2 mCi), 71 ± 3 MBq (2 mCi), and 132 ± 3 MBq (3.6 mCi) was administered to patients in groups 1, 2, and 3, respectively. Each syringe was assayed in a dose calibrator (Curiementor 3; PTW) before and after dose administration, and the administered activity value was the difference between the values.

TABLE 1
Patient Characteristics

Patient no.	Age (y)	Sex	Weight (kg)
1	45	F	76
2	46	M	68
3	52	F	54
4	29	F	58
5	18	F	43
6	49	M	123
7	74	M	116
8	18	M	49
9	50	F	70
10	43	F	66
Mean ± SD	42.4 ± 16.9		73.5 ± 26.8
11	35	F	73
12	20	F	57
13	40	F	61
14	35	M	78
15	44	F	59
16	42	M	67
17	51	F	85
18	29	F	54
19	52	F	61
20	55	F	67
Mean ± SD	40.3 ± 10.9		66.2 ± 9.8
21	19	M	83
22	31	F	66
23	68	M	55
24	55	M	81
25	37	F	41
26	38	F	50
27	18	F	64
28	46	F	44
29	65	F	54
30	38	F	64
Mean ± SD	41.5 ± 17.2		60.2 ± 14.2

Scintigraphy

A digital single-head γ-camera (model 1000, circular DCX; Sopha) was used. It was equipped with a general-purpose parallel-hole collimator (HRBE8-140). The γ-camera was calibrated by the National Electrical Manufacturers Association protocol and interfaced to a computer. During the hour before the investigation, the patients were hydrated according to a standard scheme. They were positioned supine under the collimator and imaged. Dynamic images were acquired in 2 phases: sixty 1-s frames and sixty 30-s frames. A matrix size of 128×128 pixels was used with a 10% energy window about the 140-keV photopeak. Time–activity curves were generated from manually drawn regions of interest (ROIs) over the kidneys, the cortex, and semilunar background regions adjacent to the kidneys (including parts of the liver or spleen). The background was normalized to the area of the kidney ROIs using the protocol for the Sopha γ-camera, and the background count was subtracted from the kidney counts. The uptake phase in the renograms was defined as the linear part of the renogram before outflow started. ERPF, in percent, was calculated from the total number of counts during the uptake phase (i.e., the first 2 min after administration, not affected by excretion) (5). The number of counts in each ROI was quantified.

A series of images of perfusion and clearance was obtained from each patient. An expert observer who did not know the administered activity evaluated the images. The observer subjectively graded the image quality as good (5 points), fair (4 points), or poor (3 points).

The processed quantitative parameters included the uptake time from the renogram of the left and right kidneys (TM_{LK} and TM_{RK}, respectively), the counting rate 2 min after injection, the labeling yield, the percentage of the injected activity in the left and right kidneys 2 min after injection ($A2_{LK}$ and $A2_{RK}$, respectively), and ERPF for both kidneys. In addition, the selected ROIs were processed as ratios of counts in the left and right kidneys to the background (LK/B and RK/B, respectively) and in the left and right cortex to the background (LC/B and RC/B, respectively), taking into account subtraction of the background from the kidney and cortex counts. The ROIs were traced over the image corresponding to 2 min after injection. Table 2 shows the results of all these parameters. Statistical Package for Social Sciences, version 9.0 (SPSS Inc.), was used to apply the clustering techniques and the discriminant analysis to the collected data.

Mathematic Optimization Procedure

Clustering techniques are particularly useful when levels of image quality cannot be differentiated by simple observation (6), such as when noise levels are similar among images. In these cases, the normal distributions of signal plus noise between any pair of images overlap by more than 2 SDs. For this reason, the observer affirmed that all the images are of similar quality (7). Nevertheless, the differentiated groups can be discerned mathematically on the basis of the measured variables.

TABLE 2
Measured Variables

Patient no.	TM$_{LK}$ (min)	TM$_{RK}$ (min)	Counting rate (cps)		LY (%)	LK/B	RK/B	LC/B	RC/B	A2$_{LK}$ (%)	A2$_{RK}$ (%)	ERPF (%)	
			Left	Right								Left	Right
1	2.7	2.0	248	248	90	4.6	4.0	3.8	2.5	11.8	13.5	46	54
2	2.3	3.1	186	284	90	4.2	5.2	2.9	4.1	11.0	16.7	42	58
3	3.5	1.5	325	99	90	3.0	1.0	2.4	0.5	21.1	6.43	92	8
4	10.5	30	232	285	87	2.7	3.5	2.7	3.0	14.1	17.1	72	20
5	3.7	2.6	326	459	87	4.0	3.5	3.3	3.0	23.0	28.0	43	57
6	2.6	3.7	157	88	87	3.4	4.2	3.0	3.2	11.4	5.92	92	8
7	24	18	166	226	91	3.9	2.0	3.7	1.6	9.58	14.1	39	61
8	—	7.5	272	229	91	—	3.0	—	2.4	—	19.3	—	98
9	2.2	2.5	170	215	91	5.4	4.3	4.4	3.8	13.1	14.2	48	52
10	3.8	3.6	161	223	90	4.7	4.6	4.3	4.2	13.1	13.6	51	49
11	2.7	—	262	—	90	6.8	—	5.2		19.9	—	96	—
12	30	5.6	243	131	91	6.8	1.8	6.2	1.5	25.8	27.3	36	64
13	2.1	—	164	—	91	3.3	—	2.9	—	13.6	—	94	—
14	6.3	—	216	—	91	11.1	—	9.2	—	18.7	—	93	—
15	21.6	13.9	106	200	87	3.2	2.8	2.7	2.1	7.5	15.2	29	71
16	18.7	17.2	107	81	90	1.7	2.3	1.4	2.0	6.6	15.8	15	85
17	2.7	3.4	86	216	90	1.9	1.8	1.8	1.3	8.6	6.4	58	42
18	2.8	3.7	241	70	90	3.6	0.7	3.4	0.4	19.0	55.3	85	15
19	—	5.6	113	94	90	—	2.5	—	1.9	—	11.2	—	99
20	17.6	3.7	221	206	90	7.0	3.1	6.5	2.7	13.2	17.4	53	47
21	1.9	1.8	45	193	90	0.7	3.3	0.7	3.3	7.6	47.4	19	87
22	3.2	3.4	151	201	88	4.6	4.2	4.1	4.2	17.8	23.6	23	77
23	2.8	2.8	36	206	88	0.3	2.9	0.2	2.8	4.5	25.2	7	93
24	2.8	1.8	136	137	88	5.2	2.2	4.6	2.0	17.1	16.9	48	52
25	2.5	10.5	268	94	90	6.9	1.9	6.6	1.6	28.2	9.9	90	10
26	3.0	7.5	239	65	90	7.7	0.6	6.8	0.5	25.1	6.7	90	10
27	1.9	1.9	213	210	90	4.3	3.2	4.1	2.5	20.0	20.0	51	49
28	2.2	2.7	179	130	90	4.1	1.4	3.5	0.9	22.6	16.9	60	40
29	20.2	5.2	27	142	90	0.9	2.5	0.9	2.2	18.9	9.2	16	84
30	2.9	3.7	130	108	90	3.2	1.8	2.9	1.6	16.7	15.1	60	40

LY = labeling yield.

Patients 8, 11, 13, 14, and 19 had only 1 kidney. Counting rate is at 2 min after injection.

The centroids of both groups (clusters) are the mean values of the measured variables in the differentiated groups. The process is as follows:

From the initial data matrix (D), which is obtained from the measured variables for the number of analyzed cases (N_c), the distance between each pair of cases can be calculated by the traditional Euclidean distance (8):

$$D_{A,B} = ((X_{A1} - X_{B1})^2 + (X_{A2} - X_{B2})^2 + \ldots (X_{Ai} - X_{Bi})^2)^{1/2}, \qquad \text{Eq. 1}$$

where X_{A1} to X_{Ai} are the values of each of the X_i measured variables of one case and X_{B1} to X_{Bi} are the values of each of the X_i measured variables of another case.

The k-means clustering method chooses a specified number of cluster centroids (2 in our model). The 2 cases with the highest distance in the matrix D are selected. The values of these variables for these extreme cases are considered the initial centroids of the initial clusters. The distances to both centroids are calculated for each case. Each case is then placed in the cluster whose distance to the centroid is the lowest. Finally, the centroids are recalculated for each cluster among all the cases. Under these conditions, it can be assumed that each cluster has a different level of image quality according to the X_i measured variables.

The linear discriminant analysis is then used for the above clusters. The objective is to construct an image-quality discriminant function that selects, from all the measured variables (X_i), those that truly differentiate groups by image quality (X_{n*}).

The form of the function is:

$$z = \lambda_1 X_1 + \lambda_2 X_2 + \ldots \lambda_{n*} X_{n*}, \qquad \text{Eq. 2}$$

where X_i is a variable, λ_i is a constant coefficient, and z is the discriminant punctuation of each case.

The λ_s values are calculated from n* linear equations (7):

$$\lambda_1 \sigma_{11} + \lambda_2 \sigma_{12} + \ldots \lambda_{n*} \sigma_{1n*} = \mu_{11} - \mu_{21}$$

$$\lambda_1 \sigma_{21} + \lambda_2 \sigma_{22} + \ldots \lambda_{n*} \sigma_{2n*} = \mu_{12} - \mu_{22}$$

$$\lambda_1 \sigma_{n*1} + \lambda_2 \sigma_{n*2} + \ldots \lambda_{n*} \sigma_{n*n*} = \mu_{1n*} - \mu_{2n*}, \qquad \text{Eq. 3}$$

where σ_{kp} (k,$P = 1...n^*$) are the covariance element matrix corresponding to the X_{n^*} variables. They are calculated as:

$$\sigma_{kp} = \sum_{i=1}^{N_c} (X_{ki} - \bar{X}_k)(X_{pi} - \bar{X}_p), \qquad \text{Eq. 4}$$

and μ_{ij} are the mean values of each of the selected variables, where i takes the values 1 or 2 (groups) and $j = 1...n^*$.

Depending on the z value ($z < C$ or $z > C$), each case is classified into one or the other cluster according to the new selected variables X_{n^*}. C is considered the threshold between clusters. It might not be determined visually but can be calculated as:

$$C = (\bar{z}_N + \bar{z}_A)/2, \qquad \text{Eq. 5}$$

where $\bar{z}_N$ and $\bar{z}_A$ are the discriminant punctuations for both final groups according to the X_{n^*} discriminant variables.

The correlation factors for each selected variable are calculated. A weighting factor for each variable is established on the basis of its relevance for image-quality discrimination.

To reduce the number of variables relevant to image quality from the initial measured X_i to the final X_{n^*}, correlation factors are calculated among all the variables, following their order of relevance for image quality. Just those variables with the highest relevance for image quality are included in the function. The function is formed from variables with no correlation or with a poor correlation ($r < 0.2$) (*8*). The rest of the variables are neglected. The selected variables are those that cannot be extracted from the function without affecting the percentage of cases correctly classified into the groups with differentiated image quality. The minimum value of the administered activity, among a group of tested activities that still yield good results for the (X_{n^*}) selected parameters, can then be assumed the optimal choice.

Usually, the most important product of γ-camera renography is not the image itself but the time–activity curves that can be generated from the images to evaluate renal function. In this sense, the activity that yields good results for the image-quality parameters has to be an activity that also generates adequate time–activity curves and determines ERPF with adequate precision (*3,4*). In the present work, the possible association between the administered activity and the main parameters obtained from the curves (precision in ERPF determination, TM_{LK} and TM_{RK}, and $A2_{RK}$ and $A2_{LK}$) was also analyzed.

RESULTS

The ERPF of both kidneys was calculated 15 times for each patient to find the precision of the calculation from manually determined ROIs. The results were analyzed to determine whether the precision depended on the administered activity, and they were compared with reported results (*3,4*). The obtained SDs varied by ±1.5% for 132 MBq, ±1.7% for 71 MBq, and ±2.0% for 45 MBq. The values were not significantly different at a 95% confidence level

($P = 0.09$). This level of precision did not correlate with the activity in the right or left kidney ($r = 0.144$ and $r = 0.151$, respectively). The measured parameter that best correlated with precision in the ERPF determination was the counting rate 2 min after injection ($r = 0.467$ for the left kidney and $r = 0.419$ for the right kidney).

The observer graded the quality of all sets of images as good (5 points). Nevertheless, 2 differentiated clusters of image quality were mathematically identified (Table 3) on the basis of the following parameters: the ratios LK/B, LC/B, RK/B, RC/B; $A2_{LK}$ and $A2_{RK}$; and the main labeling yield. Figure 1 shows an example of images obtained with each administered activity level and their corresponding renograms for both whole kidneys.

Based on the above classification, the constructed discriminant function of image quality was:

$$IQ = 0.25LY + 2.27\frac{LK}{B} + 2.47\frac{RK}{B} - 2.47\frac{LC}{B}$$

$$+ 1.74\frac{RC}{B} + 0.26A_{2LK} - 0.26A_{2RK}, \qquad \text{Eq. 6}$$

where IQ is z (discriminant punctuation of each case according to the selected variables) and LY is labeling yield.

The function classified 89% of the patients correctly. The correlation coefficient of each variable with the function is shown in Table 4. Introduction of the weight, age, or sex of the patient into the function did not change the percentage of correct predictions among the patients. Nevertheless, the above variables cannot be extracted without affecting the percentage of patients correctly classified into the clusters.

Of the parameters selected by the discriminant function, the only one that showed significant differences with the variation in administered activity was the RK/B ratio ($P = 0.026$), but the significance was not strong. In this case, the differences were subtle between 45 MBq (1.2 mCi) and 132 MBq (3.6 mCi) ($P = 0.035$) and between 71 MBq (2 mCi) and 132 MBq (3.6 mCi) ($P = 0.019$), with better results for 132 MBq (3.6 mCi) in general.

No correlation was found between the administered ac-

TABLE 3
Clusters with Differentiated Image Quality

Variables	Value in cluster 1	Value in cluster 2	Patient classification in cluster 1	Patient classification in cluster 2
LK/B	3.83	4.01		
LC/B	3.23	3.62		
RK/B	2.42	3.39	3, 6, 12, 17, 18, 19,	1, 2, 4, 5, 7, 8, 9,
RC/B	2.06	2.75	24, 25, 26, 28, 29,	10, 15, 16, 20, 21,
A2$_{LK}$ (%)	15	18	30	22, 23, 27
A2$_{RK}$ (%)	16	18		
Labeling yield (%)	90	92.3		

The software could not classify patients 11, 13, and 14.
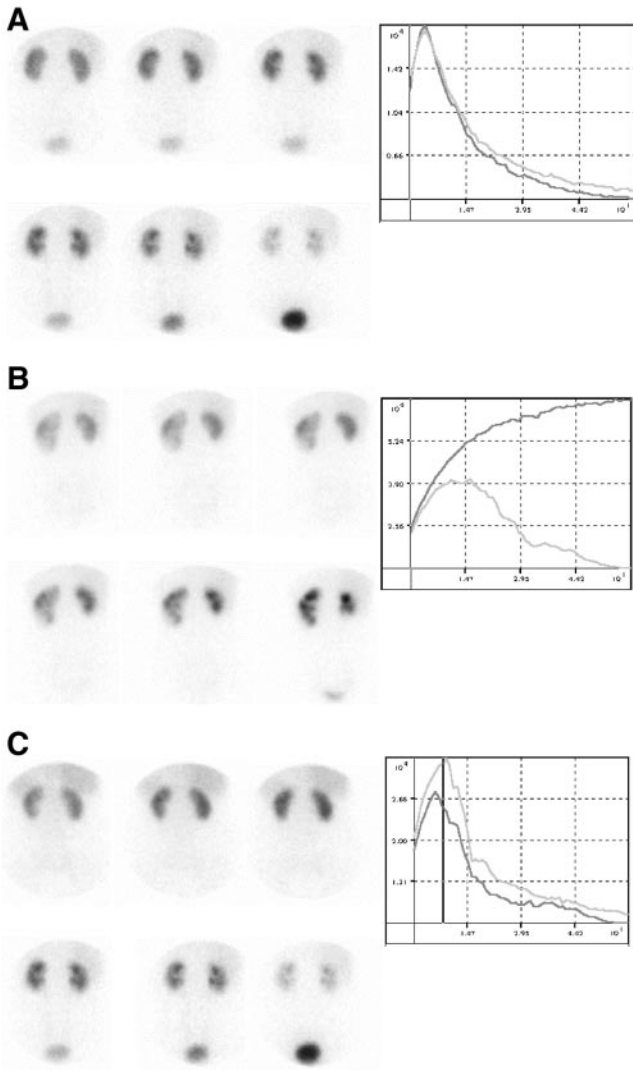
FIGURE 1. Images obtained with 45 MBq (A), 71 MBq (B), or 132 MBq (C) of ^{99m}Tc-MAG3 and their corresponding renograms for both whole kidneys.

tivity and the remaining main parameters of the time–activity curves: TM_{LK} ($r = 0.15$), TM_{RK} ($r = 0.13$), $A2_{LK}$ ($r = 0.21$), and $A2_{RK}$ ($r = 0.30$).

MIRDOSE3 was used to calculate the absorbed doses in some relevant organs after administration of 3 different

activity values (a value commonly used in our practice, the value recommended by the International Atomic Energy Agency (IAEA), and the optimized value obtained from this study). The results are presented in Table 5. The residence times were taken directly from Report 53 of the International Commission on Radiological Protection (9).

DISCUSSION

The relationship between the amount of radiopharmaceutical administered to patients and its effect on image quality has yet to be fully studied. The amount of activity administered varies among centers and is not always based on optimization criteria that look for a compromise between image quality and the radiation protection of the patient. For dynamic renal studies using ^{99m}Tc-MAG3, the maximum value reported is 1,000 MBq (27 mCi) (10). A value of 100 MBq (2.7 mCi) has been recommended as being adequate and having a high safety margin (3,4,9,11,12). The maximum value recommended by the IAEA for adults is also 100 MBq (2.7 mCi) (1). This value has been reduced in some centers to 45 MBq (1.2 mCi) (3,4) according to the equipment being used.

Some authors have maintained that more than 200 MBq (5.4 mCi) are needed to achieve good-quality perfusion images (13). The mean value used in some European countries is 90 MBq (2.4 mCi) (10). International organizations recognize the reasonability of determining the appropriate administered activity by optimization procedures (1,14). The activity administered in each center depends on the radiopharmaceutical choice, equipment characteristics, matrix size, patient size, acquisition time, and study type (static, dynamic, or SPECT) (2). In our study, all parameters except patient characteristics, labeling yield, and administered activity were kept fixed.

The 3 activities administered in this study generated time–activity curves (renograms) that had few changes in the statistical noise (error less than 2%). Statistical noise in time–activity curves depends on the total count in γ-camera renograms and is based mainly on the amount of activity in the kidneys and background. Vestergren et al. (4) found that the

TABLE 4
Importance of Variables for Image Quality

Rank from highest to lowest importance	Correlation coefficient with discriminant function
RK/B	0.646
RC/B	0.467
$A2_{RK}$	0.290
$A2_{LK}$	0.162
Labeling yield	0.137
LK/B	0.035
LC/B	0.029

TABLE 5
Absorbed and Effective Doses in Some Organs After Different Administered Activities of ^{99m}Tc-MAG3

Organ	Administered activity		
	185 MBq (common value)	100 MBq (IAEA value)	45 mBq (optimized value)
Absorbed dose (mGy)			
Red marrow	3.30	1.80	0.80
Kidneys	33.30	18.00	8.10
Bladder	32.37	17.50	7.87
Liver	9.25	5.20	2.20
Ovaries	2.22	1.20	0.54
Testes	1.11	0.60	0.27
Whole body	1.10	0.59	0.26
Effective dose (mSv)	4.86	2.64	1.17

counting rate 2 min after injection is the main determinant of the precision of ERPF calculation. We found a correlation between the precision of ERPF determination and the counting rate 2 min after injection. Nevertheless, from our data, although counting rate clearly depended on administered activity, precision in ERPF determination showed just a weak linear dependence on activity range (from 1.5% for 132 MBq to 2% for 45 MBq). For this reason, precision in determining ERPF depended more on precision in manually selecting the ROIs than on the activity administered.

Although the most relevant aspect of this kind of nuclear dynamic study is the generation of renograms with little statistical noise, so that ERPF can be determined with good precision, we also analyzed the quality of perfusion and clearance images because it affects the interpretation of time–activity curves. It is important to evaluate whether activity reduction degrades image quality.

The ratios RK/B and RC/B were the most important parameters affecting discrimination between the 2 differentiated clusters of image quality. These ratios were very different in relevance with respect to their homologues (LK/B and LC/B), because decreasing the labeling yield at the expense of colloid formation leads to an increase in liver uptake that, in turn, affects image quality. In this research, the main labeling yield did not greatly affect discrimination, because the collected data for this variable varied only slightly. Nevertheless, the mean value for this parameter was 92.7%, which is not considered high.

From Table 3, one can see that cluster 2 included the patients with better image quality. The parameters more relevant to image quality had higher values for the patients in this cluster. Nevertheless, only RK/B was significantly different between the 2 clusters. The differences in image quality associated with the selected parameters were, in general, very small between the 2 clusters. These small differences were not enough to be seen by the observer. This method is more sensitive for the detection of small changes than is subjective evaluation by an expert.

Our study showed that reduction of the administered activity to 45 MBq (1.2 mCi) is sufficient, provided that a high labeling yield is guaranteed and, thus, significant differences among the images according to the ratio RK/B are avoided. This result is in line with the results of a previous study (4) in which the background was not negligible.

Because the variation in administered activity in this study was small, this evaluation might appear to not be essential. However, a reduction in administered activity leads to a reduction in the absorbed radiation dose to the patient, particularly to the bladder and kidneys. Our study showed that the effective dose, a parameter commonly used to assess radiation risk (15), was reduced as a result of small reductions in administered activity.

CONCLUSION

This study showed that radiation risk can be reduced without affecting the quality of the diagnostic information.

This finding may be particularly relevant for patients who undergo frequent nuclear medicine studies to follow the disease. A reasonable compromise between image quality and radiation protection must be achieved. The use of a discriminant function is a fast and easy method of optimizing studies by determining which variables affect image quality. The administered activity of ^{99m}Tc-MAG3 can be reduced to 45 MBq (1.2 mCi) as long as a high labeling yield for the MAG3 is guaranteed. Precision in the determination of ERPF is not significantly affected by a reduction in the administered activity to 45 MBq (1.2 mCi). The method is a fast and easy way to find the optimum level of administered activity and can be applied in any department of nuclear medicine according to its specific technical conditions.

REFERENCES

1. International Atomic Energy Agency. *International Basic Safety Standards for Protection Against Ionizing Radiation and for the Safety of Radiation Sources.* Vienna, Austria: IAEA; 1996. Safety Series 115.
2. Oei HY. Dynamic and static renal imaging. In: Murray IPC, Ell PJ, eds. *Nuclear Medicine in Clinical Diagnosis and Treatment.* 1st ed. New York, New York: Churchill Livingstone; 1995:213–217.
3. Moonen M, Jacobsson L. Effect of administered activity on precision in the assessment of renal function using gamma camera renography. *Nucl Med Commun.* 1997;18:346–351.
4. Vestergren E, Jacobsson L, Moonen M, Eklund I, Sixt R, Mattsson S. Administered activity of ^{99m}Tc-MAG3 for gamma camera renography in children. *Nucl Med Commun.* 1999;20:799–806.
5. Moonen M, Jacobsson L, Granerus G, Friberg P, Volkmann R. Determination of split renal function from gamma camera renography: a study of three methods. *Nucl Med Commun.* 1994;15:704–711.
6. Pérez Díaz M, Quevedo García J, Ponce Vicente F, Diaz Rizo O. Administered activity optimization in patients studied by equilibrium gated radionuclide ventriculography using pyrophosphate and Tc-99m. *Nucl Med Commun.* 2002;23:347–353.
7. Evans AL. *Evaluation of Medical Images.* Bristol, U.K.: Adam Hilger Ltd.; 1981:80–113.
8. Venables WN, Ripley BD. *Statistics and Computing: Modern Applied Statistics with S-Plus.* New York, NY: Springer-Verlag; 1994:311–318.
9. International Commission on Radiological Protection. *Radiation Dose to Patients from Radiopharmaceuticals.* Oxford, U.K.: Pergamon Press; 1988. ICRP publication 53.
10. Mattsson S, Jacobsson L, Vestergren E. The basic principles in assessment and selection of reference doses: considerations in nuclear medicine. *Radiat Prot Dosimetry.* 1998;80:23–30.
11. Taylor A Jr, Eshima D, Fritzberg AR, Christian PE, Kasina S. Comparison of iodine-131 OIH and technetium-99m MAG3 renal imaging in volunteers. *J Nucl Med.* 1986;27:795–803.
12. Jafri RA, Britton KE, Nimmon CC. Technetium-99m MAG3, a comparison with iodine-123 and iodine-131 orthoiodohippurate, in patients with renal disorders. *J Nucl Med.* 1988;29:147–158.
13. Itoh K, Tskamoto E, Kakizaki H, et al. Phase II of Tc-99m-MAG3 in patients with nephrourologic diseases. *Clin Nucl Med.* 1993;18:387–393.
14. Administration of Radioactive Substances Advisory Committee (ARSAC). *Notes for Guidelines on the Administration of Radioactive Substances to Persons for Purposes of Diagnosis, Treatment and Research.* London, U.K.: ARSAC; 1993.
15. International Commission on Radiological Protection. *Recommendations of the International Commission on Radiological Protection.* Oxford, U.K.: Pergamon Press; 1991. ICRP publication 60.